Study of Metabolic Enzyme-Efflux Transporter Relations with *in Silico* Devices

Lana X. Garmire

***Abstract*—In order to study the complex interactions and positional relations between metabolic enzymes such as CYP and efflux transporters such as PGP, we constructed an In Silico Transwell Device (ISTD) and an In Silico Intestine Device (ISID) to represent in vitro cell culture systems and human small intestines. Both are 3-dimentional, discrete event, discrete space, agent-based models. An ISID is a modification of an ISTD. To study CYP–PGP interactions, we completed 5 simulated cases using both devices. Simulation results showed: 1) with the ISTD under certain circumstances, either synergistic or antagonistic, or no effects occurred; 2) backflow occurring in the ISTD led to CYP–PGP interactions for the drugs whose CYP reaction rates are slow; whereas 3) backflow occurring in the ISTD is not an essential condition for the drugs which react quickly with CYP; and 4) CYP–PGP interactions do not occur in the ISID, suggesting that they are unlikely in human intestines. We also simulated the effect of proximity between CYP and PGP using the ISTD. The simulation results showed: (1) under the same PGP condition, transport is determined dominantly by the closeness of CYP to the membranes (either the apical membrane or the basal membrane); (2) unexpectedly, the asymmetric localization of PGP on the apical membrane does not facilitate more transport, but it slightly enhances metabolism.**

***Index Terms*—agent-based model, metabolism, synergy, transport**

I. Introduction

In the intestinal epithelium, at least two types of proteins function to decrease absorption of potentially toxic xenobiotics: phase I metabolic enzymes, such as cytochrome P450 (or abbreviated as CYP) and efflux transporters, such as P-glycoprotein (or abbreviated as PGP). CYPs are hemoproteins tethered on the endoplasmic reticulum membrane; they metabolize xenobiotics by adding polar groups. PGP are transmembrane proteins located only on the apical membrane of epithelial cells; they pump absorbed intracellular xenobiotics back into the lumen of the intestine. Some researchers suggested that PGP and CYP act synergistically to reduce the absorption of dual-substrate compounds. This is evidenced by the observation that the transport increase by inhibiting CYP and PGP together was greater than the sum of the transport increase by inhibiting CYP and PGP separately. However, the supporting results for synergy were obtained from in vitro systems or perfused intestines, where experimental conditions differed from in vivo conditions [1] [2].

Some other qualitative evidence also seems to suggest synergy between CYP and PGP. One case is the immuno -staining image of epithelial cells, which showed that CYP is preferentially located closer to the apical membrane, where PGP exists, rather than the basal membrane, where PGP does not exist [3].

Simulation is a powerful tool for gaining deeper insight into such biological complexity. Using simulated systems, we are able to study whether CYP–PGP synergy exists in vitro and in vivo, and if they do, what are the critical conditions. The answers to these questions are very attractive from a theoretical point of view. And this report is aimed to accomplish such goals.

II. Methods

The ISTD and the ISID are 3D discrete event, discrete space, stochastic models that use the synthetic modeling method. The models were coded using the Java-Swarm platform. The Java-Swarm platform gives direct access to the Swarm libraries and enables the created software to be easily integrated with statistical and mathematical software, such as R and Matlab, for post-simulation data processing.

A. Model Structures and Components

Model structure of the ISTD is shown in Fig 1. Simulated biological mechanisms of passive transport through cells and enzymatic reactions were those reported previously [5]. *DRUGS* [1] were mobile objects; *CYP* and *PGP* were not. An ISID is a modification of an ISTD. The model structure of the ISID is shown in Fig 2. There are several major differences in the ISID: (1) S1 of the ISID is a cylinder structure filled with intestinal lumen contents , unlike the flat 3-dimensional apical compartment in the ISTD, (2) the direction along the y-axis in the ISID represents the proximal → distal terminal of the intestine and as a result, S2-S5 spaces are wrapped into cylinder structures, rather than torus structures as done in the ISTD, and (3) an added bias factor, *e*, forces the biased flow along the y direction in S1 space of the ISID.

Manuscript received August 10, 2007.

L. G. Author is with the Graduate Group in Comparative Biochemistry, University of California at Berkeley, Berkeley, CA, 94530 USA (phone: 510-703-5359; e-mail: lanxia@ berkeley.edu).

1 SMALL CAPS: in silico analogues of biological referent component.

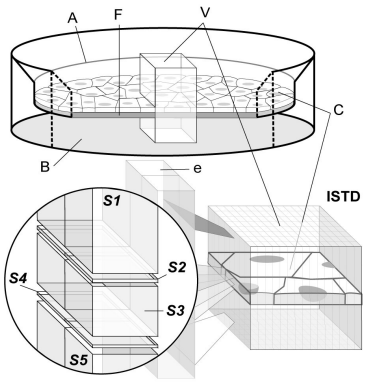

Fig 1 Top: in vitro transwell. A, B: apical, basal compartment; C: epithelial cell; F: filter; V: an arbitrary vertical column section through the system. Bottom: ISTD. e: 1/10,000 simulated 3D elements of S1; S1–S5: in silico representation of apical compartment, apical cell membranes, intracellular spaces, basolateral cell membranes, and the basal compartment of the transwell device

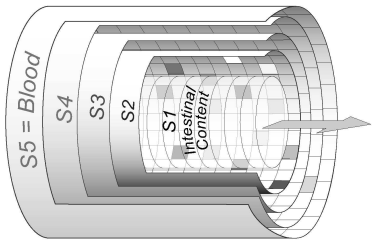

Fig 2 The structure of ISID. *S1*: intestinal content; *S2*–*S4*: the same as in Fig.1; *S5*: blood; Arrow: luminal flow direction

B. Discrete Event Schedules

Discrete event simulation can be more efficient than discrete time simulation [4]. The ISTD and the ISID simulations are advanced by dynamically scheduled discrete events occurring at realistic times. Two levels of agents manage event scheduling. At the bottom level, four scheduling agents, *Transit Event Scheduler*, *Lateral Event Scheduler, Enzyme Event Scheduler*, and *Transport Event Scheduler* control the progress of *DRUG* relocation and transition into adjacent spaces, lateral diffusion within each space, metabolism and efflux transport, respectively. Above these agents is the master *Schedule Event* agent; it coordinates the activities of the other four sub-agents.

C. Passive Diffusion

The details of Passive Diffusion were described in our previous paper [5]. Passive diffusion was composed of vertical diffusion and transition between and within spaces, and lateral diffusion within a space. Lateral diffusion was designed as a random process that obeys a Gaussian distribution. Vertical transition was achieved by a complex algorithm incorporating a series of rules (logic) based on probabilistic criteria. The rules considered events occurring transcellularly as well as in tight junctions. The validation was reported in [5].

D. Enzymatic Reaction & Efflux Transport Algorithm

Details of the enzymatic reaction were explained in the previous paper [5]. Briefly, the enzymatic reaction algorithm was a stochastic analog of the conventional kinetic model. Each *ENZYME* agent changes its state depending on the internal logic, local environment and probabilities from a pseudo-random number generator (RNG). Each *ENZYME* has two-substrate binding sites, so that the atypical self-activation and/or self-inhibition can be simulated. The logic of 2-site *ENZYME* is shown below in Fig 3. In this report, for simplicity, we inactivated site 2, so that the reactions behaved as Michaelis-Menten kinetics. Efflux transport of PGP mechanism was similar to that of enzymatic reactions, except that: (1) *PGP* released the bound substrate in its original form, instead of turning the substrate to metabolites as was done by *ENZYME*; (2) *PGP* translocated substrates into S1 (lumen) space, instead of releasing the metabolites in S3 as was done by *ENZYME*.

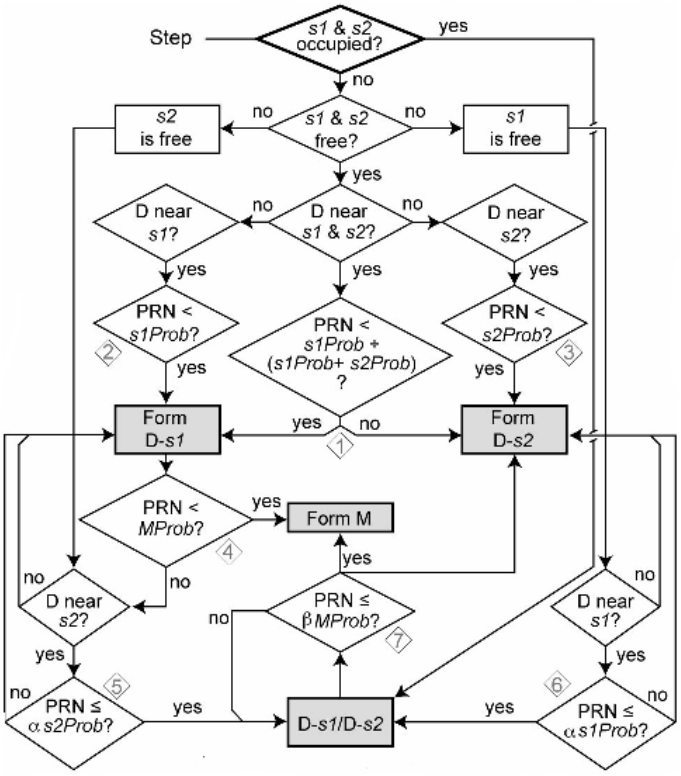

Fig 3 The logic followed by each *ENZYME* during a simulation cycle. D: *DRUG*; M: *METABOLITE*; D-*s1* (or D-*s2*): DRUG bound to *s1* (or *s2*); PRN: a uniform pseudorandom number drawn from [0, 1]. The numbers within diamonds identify seven questions, whose answer determines which, if any, state change will occur and whether the *DRUG* is converted to a *METABOLITE*.

E. CYP-PGP Interaction Experiments Set-Up

To make the results directly comparable, simulation surfaces in the ISTD and the ISID have the same width x=2π×1.5cm and length y=5cm. All simulations were initiated with 1000 *DRUG* agents (MW=150, logP=2 pKa=6.5, base) in S1. The numbers of *DRUG* agents transported were collected in S5. All simulations use the same numbers of *CYP* (n=480) and *PGP* (n=419). They follow the reported in vivo distribution patterns [6] [7]. The cycling time of both *PGP* and *CYP* are set to be 5 seconds or 0.5 second, depending on the case. For simplicity, we set parameters prob. (*PGP* binds *DRUGS*) = prob. (*PGP* releases *DRUGS*) = P_1 and prob. (*CYP* binds *DRUGS*) = prob. (*CYP* releases *DRUGS*) = P_2. In this report, the values of $P_{1/2}$ = [0, 0.5, 1], total 9 combinations.

The ISTD had a grid size of 15×800. In the ISTD, *DRUG*s were seeded randomly in S1. A *DRUG* agent can randomly diffuse in S1 space in the x, y, and z directions. *CYP* and *PGP* both had a substrate detecting Moore radius=1. We collected the number of drug agents transported to S5 after simulating for 1 hour.

The ISID had a grid size of 75×4000. In the ISID 3ml of *DRUG*s were seeded at the proximal terminal in S1. We assumed

*DRUG*s were in solution and ignored the *DRUG* disassembling process. *CYP* and *PGP* both had a substrate detecting Moore radius=5, so that their effective range was the same as that in ISTD. Besides randomly diffusion in S1 space on (x, y, z) directions, luminal flow was introduced in the form of the bias factor *e*. We collected *DRUG*s excreted at the distal terminal and optimized *e*=45 by setting the mean transit time of *DRUG*s to be 3 hours.

F. CYP Localization Experiments Set Up

The ISTD had a grid size of 100×100 to represent the 4.71cm^2 transwell surface area. As the focus of the experiments was CYP localization in the cell, we eliminated the tight junction (TJ) transport by assigning TJ%=0. All simulations started with 1000 drugs (MW=500, neutral, logP=3) in S1 space, and ended at 1 hour. All simulations used the same numbers of *CYP* (n=400) and *PGP* (n=660). They both had uniform random distributions. The cycling time for both *PGP* and *CYP* were set to be 5 seconds. For simplicity, we set parameters prob. (*PGP* binds *DRUGS*) = prob. (*PGP* releases *DRUGS*) = prob. (*CYP* binds *DRUGS*) = prob. (*CYP* releases *DRUGS*) = 1. Metabolites were assumed to inherit all the physicochemical properties of parent drugs. For simplicity, we assumed metabolites were neither substrates of PGP nor CYP.

III. Results

A. Model Validation

The validity of the passive diffusion module and enzymatic reaction module of the ISTD were shown in [5]. Before we used the ISTD and ISID to study relations of CYP–PGP, we first illustrated the applicability of the full model ISTD to drug transport in general. We chose Sirolimus (MW=914, pKa=10.4, logP= 5.773, base), a dual substrate of CYP and PGP, as an example. As shown in Fig 4, during the 3 hours course, the simulation results are very close to the experimental results of Cummins *et al.* [8].

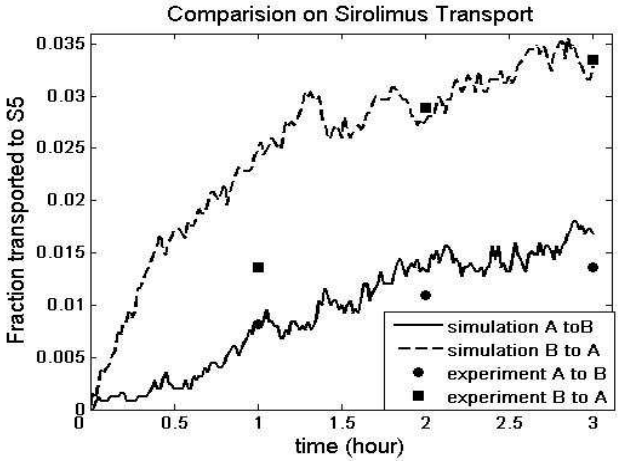

Fig 4 Comparison of Sirolimus transport between ISTD and experiment. Solid dots are the means (n=3) of experimental transport results from [8]. (■) drug was dosed in the apical compartment, and collected in the basal compartment; (●) drug was dosed in the basal compartment, and collected in the apical compartment. Curves are the means (n=5) of simulated results from ISTD. (–) *DRUG* was dosed in S1 and collected in S5; (--) *DRUG* was dosed in S5 and collected in S1.

B. Results on Dual Substrate Mediated CYP–PGP Interactions from Five Cases

Table I shows the major parameters for the 5 cases studied. For the in vitro simulations, backflow was allowed from S5 to S1, but no luminal flow existed in S1; for the in vitro-in vivo simulations, neither backflow nor luminal flow was allowed; for the in vivo simulations, luminal flow was allowed but not backflow. In each case, we conducted nine probabilistic parameter combinations between *PGP* and *CYP*. In each combination, we ran 10 repetitions. In the following, we describe the results of these 5 cases in order.

Table I Cases in the study

Case	condition	luminal flow	backflow	CYP/PGP cycling time (sec)
1	In vitro	no	yes	5
2	hybrid	no	no	5
3	hybrid	no	no	0.5
4	In vivo	yes	no	5
5	In vivo	yes	no	0.5

Table II shows the two-way ANOVA analysis of the effect of *PGP*, *CYP,* and their interactions on transport, using the ISTD. All three P-values are much smaller than the significance level (α=0.01), indicating that *PGP, CYP,* and their interaction effects all contribute significantly to the transport. To further explore the types of interactions between *PGP* − *CYP*, we list the mean transport data in table III.

Table II Case One ANOVA (α=0.01)

source	SS	df	MS	F	Prob>F
PGP	9243	2	4621.5	17.56	4.61e-07[a]
CYP	15482	2	7741.1	29.42	2.49e-10[b]
interaction	6561.5	4	1640.4	6.23	2.00e-04[c]
error	21313	81	263.12		
total	52599	89			

Model: Data= *PGP* effect + *CYP* effect + interaction effect +error
a: reject the null hypothesis that *PGP* has no effect on transport
b: reject the null hypothesis that *CYP* has no effect on transport
c: reject the null hypothesis that *PGP* and *CYP* do not interact

Table III Mean transport data in case one

P_2 \ P_1	0.0	0.5	1.0
0.0	390.5 [S] (E:386.9)	376.1 [A] (E:417.1)	374.6
0.5	356.0 [n] (E:356.5)	374.6 [A] (E: 386.7)	344.2
1.0	343.2	373.4	330.9

E: expected transport if *CYP* and *PGP* do not interact (e.g. 386.9 = 374.6 + 343.2 -330.9). [S]: synergy; [A]: antagonism [n]: no interaction

When neither *PGP* nor *CYP* was inhibited (P1= P2=1), 33.48% drugs were transported; when *PGP* was fully inhibited (P1=0), there was 0.2% increase of the transport, and when *CYP* was fully inhibited (P2=0), there was 4.24% increase of the transport. Assume no *CYP* – *PGP* interaction, the expected

transport when both *PGP* and *CYP* were fully inhibited should be (33.48+4.24+0.2) %=37.92%. However the observed transport was 38.99%, 2.82% higher than the expected transport, indicating synergistic interactions consistent with the previous report [9]. However, we also observed antagonistic interactions: when *PGP* was only partially inhibited (P1=0.5), but *CYP* was completely (P2=0) or partially (P2=0.5) inhibited, as shown in table III. Also no significant interactions appeared, when *CYP* was partially inhibited, but *PGP* fully inhibited. The complex results suggest that when there is backflow as in vitro conditions, interactions can appear either in the form of synergy or in the form of antagonism, mainly depending on the degrees of inhibitions on *PGP*.

Some researchers have raised the question that the synergistic interactions observed in vitro could be an artifact due to the significant backflows occurring in the in vitro system, unlike in the intestines. To test this hypothesis, we terminated the backflow in S5 of the ISTD. This scenario mimics the in vivo absorption: once a drug molecule appears in the blood, it circulates with the blood flow and does not re-renter the epithelial cells. We set the substrate- *CYP* turn-over rate slow (*CYP* cycling time=5 seconds) and conducted similar experiments as before. Two-way ANOVA analysis on transport data shows no significant contribution from either *CYP* effect or *CYP – PGP* interaction effect. The result suggests that backflow does cause *CYP – PGP* interactions for some drugs.

Table VI Case Two ANOVA (α=0.01)

source	SS	df	MS	F	Prob>F
PGP	7029.1	2	3514.5	19.05	1.6566e-07
CYP	589.6	2	294.8	1.60	0.2086[d]
interaction	1165.2	4	291.3	1.58	0.1878[e]
error	14944	81	184.5		
total	23728	89			

[d]: fail to reject the null hypothesis that *CYP* has no effect on transport
[e]: fail to reject the null hypothesis that *PGP* and *CYP* do not interact

If the turn-over rates between the enzyme/ transport and substrates are much greater than the range of the parameter values in case two, are interactions still possible even if there is no backflow? To answer this question, we speed up the *CYP* / *PGP* simulation cycle to be t=0.5 second in the ISTD and repeated experiments as in Case two. Under the new conditions, we observe that not only *PGP* and *CYP* themselves, but also their interactions contribute significantly to transport (table V). However, further analysis reveals that the interactions under such conditions are antagonistic instead of synergistic (table VI).

Table V Case Three ANOVA (α=0.01)

source	SS	df	MS	F	Prob>F
PGP	20506	2	10253	74.07	0[f]
CYP	15373	2	7686.7	55.53	6.6613e-16[g]
interaction	8363.2	4	2090.8	15.10	2.8905e-9[h]
error	11213	81	138.43		
total	55456	89			

[f]: reject the null hypothesis that *PGP* has no effect on transport
[g]: reject the null hypothesis that *CYP* has no effect on transport
[h]: reject the null hypothesis that *PGP* and *CYP* do not interact

Table VI Mean transport data in case three

P_2 \ P_1	0.0	0.5	1.0
0.0	761.0 [A] (E: 774.1)	746.2 [A] (E: 800.9)	740.9000
0.5	736.1 [A] (E: 740.4)	747.5 [A] (E: 767.2)	707.2000
1.0	719.7	746.5	686.5000

The previous scenarios all mimicked the situation that S1 does not have luminal flow, which is not true in vivo. We next introduced a bias factor *e* in S1 of the ISID to simulate intestinal flow. We analyzed the results at 3 hours, when the maximum of drug excretion rate was reached [10]. Case four represents slow *CYP* -substrate reaction rate, with the *CYP* cycling time t=5 seconds. As shown in table VII, the P-value (0.6158) of *CYP – PGP* interactions is much greater than the significance level α=0.01. It is also much larger than any other interaction P-value of previous simulations, indicating that the evidence for interactions is lacking. We also speed up the reaction turn-over rate between *CYP* -substrate and set *CYP* cycling time t=0.5 second. More extreme than the result in case four, we obtained an even larger P-value (0.8704), which indicates no evidence of *CYP – PGP* interactions (table VIII).

Table VII Case Four ANOVA (α=0.01)

source	SS	df	MS	F	Prob>F
PGP	3142.	2	1571.1	5.7671	0.0067
CYP	2414.2	2	1207.1	4.4309	0.0190
interaction	732.09	4	183.02	0.6718	0.6158[i]
error	9807.2	36	272.42		
total	16096	44			

Table VIII Case Five ANOVA (α=0.01)

source	SS	df	MS	F	Prob>F
PGP	1856.6	2	928.29	2.1177	0.1351
CYP	3918.0	2	1959.0	4.4690	0.0185
interaction	541.02	4	135.26	0.3086	0.8704[i]
Error	15781	36	438.36		
Total	22096	44			

[i]: fail to reject the null hypothesis that *PGP* and *CYP* do not interact

C. Results on Dual Substrate Mediated CYP –PGP Interactions from Five Cases

Some researchers proposed that vertical proximity of CYP to PGP is one reason to explain the synergy between CYP and PGP. In other words, as CYP is located closer to the apical membrane, the permeability of the drug decreases.

To test this hypothesis, we subdivided S3 space in the ISTD into 1000 equally spaced compartments along the vertical direction. We arbitrarily assigned the vertical substrate-detect range of *PGP* to be the top-most compartment in S3. We assigned the vertical substrate-detect range of *CYP* to be one compartment distance. We randomly seeded the *CYP* in the top most, 333rd, 666th or the bottom most compartment in S3 space. We ran 10 repetitions in each condition and compared the data collected at 1 hour. The results are shown in Fig 5 and 6.

As expected, *PGP* causes decrease in transport, drug cellular accumulation and metabolite production (Fig 5A, B, C and Fig 6). Surprisingly, the localization of *PGP* on apical membrane does not lead to more transport, comparing when *CYP* is closer to the apical membrane to when *CYP* is equally distant from the basal membrane (Fig 6). This was further confirmed by one-way ANOVA (P-value=0.6572, data not shown). But *PGP* on apical membrane does facilitate more production of metabolites, comparing when *CYP* is closer to the apical membrane to when *CYP* is equally distant from the basal membrane (Fig 6). The proximity of *CYP* to the apical membrane also has some other effects. The closer *CYP* is to the membranes (either apical or basal membrane), the lower the transport is (Fig 5A), the lower the cellular drug accumulation is (Fig 5B) and the more metabolites it can produce (Fig 5C and Fig 6).

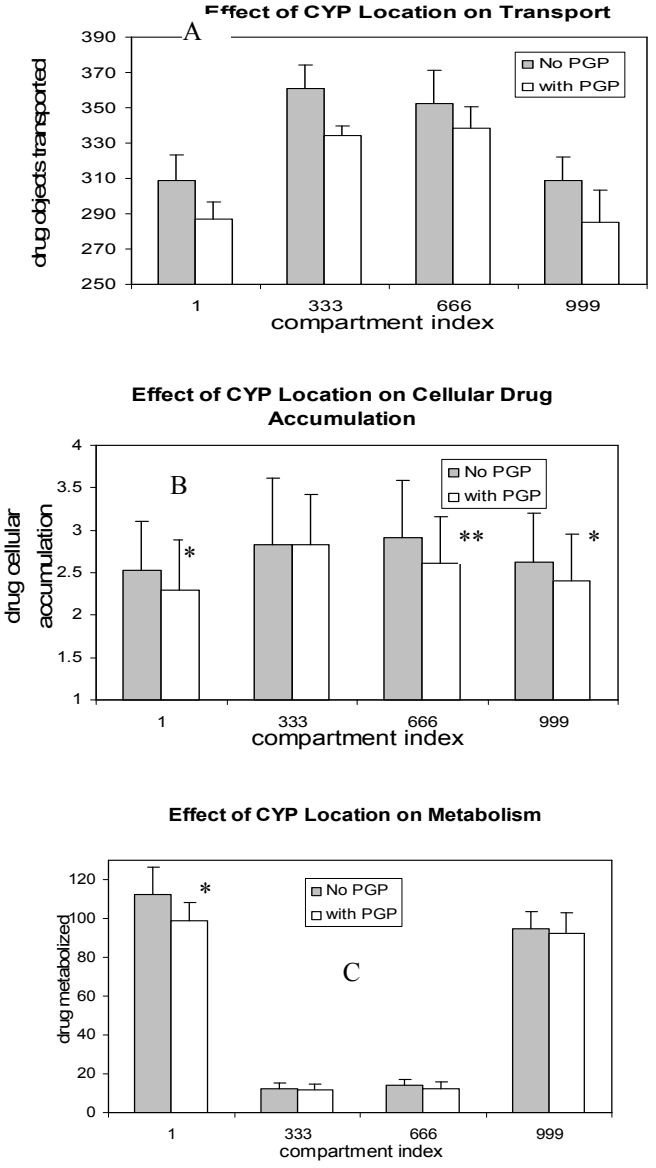

Fig 5 Effect of CYP location on A: transport, B: cellular drug accumulation and C: drug metabolism. The data are means from 10 repetitions at the end of one hour, and the error bars are the standard deviation. Gray bars represent no PGP conditions, and empty bars represent the conditions with PGP on the apical membrane. The x-axis is the index of the compartment from apical membrane. In A: Y-axis is the number of drug objects transported. In B: Y-axis is the number of drug objects accumulated in cells. In C: Y-axis is the number of drug objects metabolized in cells *: significantly different at α=0.05 level between "No PGP" and "with PGP" conditions, under the same CYP location. **: significantly different at α=0.01 level between "No PGP" and "with PGP" conditions, under the same CYP location.

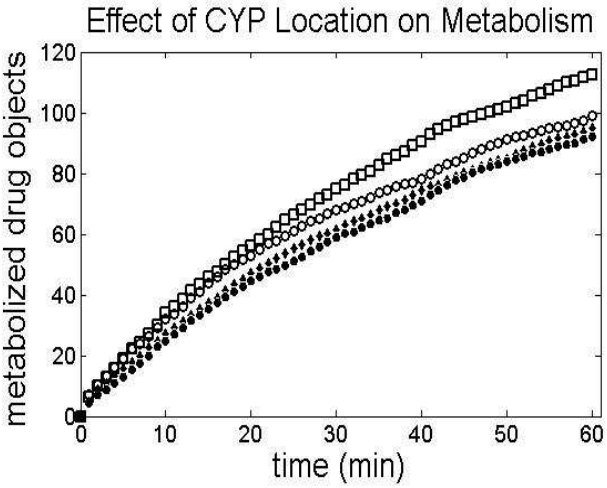

Fig 6 Time course plot of CYP positional effect on metabolism. The data are means from 10 repetitions. Empty marks are results of CYP in the 1st compartment: (□) without PGP, (○) with PGP. Solid marks are results of CYP in 999th compartment: (♦) without PGP, (●) with PGP.

IV. Conclusion

We present a new class of in silico devices ideal to aid hypothesis testing in biomedical research. Utilizing two in silico devices, the ISTD and the ISID, we conducted 5 case studies on metabolic enzyme-efflux transporter interaction problems. We confirmed that under some circumstances, synergistic CYP–PGP interaction occurs in the in vitro simulation. However, we also identified that antagonistic CYP–PGP interaction and no CYP–PGP interaction can also happen under some other circumstances in the in vitro simulation. More over, we identified that backflow occurring in the in vitro simulation could lead to CYP–PGP interactions for the drugs whose reaction rates with CYP are small; but it is not a must-have condition for the drugs which react with CYP quickly. We did not find CYP–PGP interactions occur in the ISID, inferring that they are unlikely to occur in human intestines. We also studied the effect of CYP positional proximity to PGP. Contrary to the hypothesis that vertical proximity of CYP to PGP leads to synergy in drug transport, our simulation results showed that the asymmetric localization of PGP on apical membrane does not facilitate more transport, but more metabolism, comparing when CYP is close to apical membrane to when CYP is equally close to the basal membrane. Consistent with other reports, the results confirmed the role of PGP in decreasing transport, intracellular drug accumulation and metabolism. The results also confirmed the effect of CYP proximity to membranes on decrease of drug transport and metabolism, but increase of intracellular drug accumulation.

ACKNOWLEDGMENT

The author thanks David Garmire for his help on the software techniques, and comments on the manuscript, and Anthony C. Hunt for providing sketches of figure 1 and 2.

REFERENCES

[1] L. Z. Benet, C. L. Cummins, C. Y. Wu, Unmasking the dynamic interplay between efflux transporters and metabolic enzymes. *Int J Pharm.* 2004. 277(1-2):3-9.

[2] L. Z. Benet, C. L. Cummins, C. Y. Wu, Transporter-enzyme interactions: implications for predicting drug-drug interactions from in vitro data. *Curr Drug Metab*. 2003. 4(5):393-8.

[3] P. B. Watkins, The barrier function of CYP3A4 and P-glycoprotein in the small bowel *Advanced Drug Delivery Reviews*, 1997, 27(2-3): 161-170.

[4] P. Ball, Introduction to Discrete Event Simulation, *2nd DYCOMANS workshop on "Management and Control: Tools in Action,"* Algarve, Portugal, 1996, pp. 367-376.

[5] L. X. Garmire, D. G. Garmire, C. A. Hunt, An in silico transwell device for drug transport and drug-drug interaction studies. *Pharm Res*, 2007. In press.

[6] S. Mouly, M.F. Paine, P-glycoprotein increases from proximal to distal regions of human small intestine, *Pharm Res*. 2003. 20(10):1595-9.

[7] M. F. Paine, M. Khalighi, J. M. Fisher, D. D. Shen, K. L. Kunze, C. L. Marsh, J. D. Perkins, and K. E. Thummel. Characterization of interintestinal and intraintestinal variations in human CYP3A dependent metabolism. *J. Pharmacol. Exper. Ther*. 1997. 283:1552–1562

[8] C. L. Cummins, W. Jacobsen, U. Christians, L. Z. Benet. CYP3A4-transfected Caco-2 cells as a tool for understanding biochemical absorption barriers: studies with sirolimus and midazolam. *J Pharmacol Exp Ther* 2004, 308(1):143-55

[9] Y. Liu, C. A. Hunt, Mechanistic study of the cellular interplay of transport and metabolism using the synthetic modeling method. *Pharm Res*. 2006. 23(3):493-505

[10] A. Kalampokis, P. Argyrakis, P. Macheras, Heterogeneous tube model for the study of small intestinal transit flow. *Pharm Res*. 1999. 16(1):87-91